# Photocurrent spectroscopy of exciton and free particle optical transitions in suspended carbon nanotube pn-junctions

Shun-Wen Chang, Jesse Theiss, Jubin Hazra, Mehmet Aykol, Rehan Kapadia, and Stephen B. Cronin

Citation: Applied Physics Letters **107**, 053107 (2015); doi: 10.1063/1.4928196
View online: http://dx.doi.org/10.1063/1.4928196
View Table of Contents: http://scitation.aip.org/content/aip/journal/apl/107/5?ver=pdfcov
Published by the AIP Publishing



# Photocurrent spectroscopy of exciton and free particle optical transitions in suspended carbon nanotube *pn*-junctions

Shun-Wen Chang,[1] Jesse Theiss,[2] Jubin Hazra,[2] Mehmet Aykol,[2] Rehan Kapadia,[2] and Stephen B. Cronin[1,2,3]
[1]*Department of Physics and Astronomy, University of Southern California, Los Angeles, California 90089, USA*
[2]*Department of Electrical Engineering, University of Southern California, Los Angeles, California 90089, USA*
[3]*Department of Chemistry, University of Southern California, Los Angeles, California 90089, USA*

(Received 30 May 2015; accepted 27 July 2015; published online 5 August 2015)

We study photocurrent generation in individual, suspended carbon nanotube *pn*-junction diodes formed by electrostatic doping using two gate electrodes. Photocurrent spectra collected under various electrostatic doping concentrations reveal distinctive behaviors for free particle optical transitions and excitonic transitions. In particular, the photocurrent generated by excitonic transitions exhibits a strong gate doping dependence, while that of the free particle transitions is gate independent. Here, the built-in potential of the *pn*-junction is required to separate the strongly bound electron-hole pairs of the excitons, while free particle excitations do not require this field-assisted charge separation. We observe a sharp, well defined $E_{11}$ free particle interband transition in contrast with previous photocurrent studies. Several steps are taken to ensure that the active charge separating region of these *pn*-junctions is suspended off the substrate in a suspended region that is substantially longer than the exciton diffusion length and, therefore, the photocurrent does not originate from a Schottky junction. We present a detailed model of the built-in fields in these *pn*-junctions, which, together with phonon-assistant exciton dissociation, predicts photocurrents on the same order of those observed experimentally. © *2015 AIP Publishing LLC*.
[http://dx.doi.org/10.1063/1.4928196]

The presence of strong Coulomb interactions has made exciton formation the dominant mechanism of optical absorption in carbon nanotubes (CNTs), rather than the formation of free electron-hole pairs. Theory has predicted exciton binding energies of 300–400 meV for CNTs with diameters on the order of 1 nm.[1] These uniquely large exciton binding energies are due to the strong spatial confinement of the 1D structure of CNTs, which result in interesting photophysics that is quite different from most known bulk materials.[2–6] Weisman and coworkers reported the first experimental study of excitons in CNTs in 2002 with the observation of photoluminescence (PL) from micelle encapsulate nanotubes using chemical surfactants.[2,7–9] It is interesting to note that photoluminescence was not observed in CNTs until 11 years after their discovery[10] because of their high surface-to-volume ratio, which makes them extremely sensitive to their environment. From these first photoluminescence spectra, it became clear that the single particle picture was not accurate in nanotubes and that excitonic effects were substantial even at room temperature. More recent studies have established the exciton diffusion length of air suspended carbon nanotubes to lie between 300 and 600 nm with a lifetime of 85 ps.[11,12] Reports of the exciton diffusion coefficient range from $D = 0.1\ \mathrm{cm}^2/\mathrm{s}$ to hundreds of $\mathrm{cm}^2/\mathrm{s}$ (Refs. 5 and 13–17) due to influence of the local environment on exciton-phonon scattering.[18]

Lee and coworkers measured the photocurrent spectra of a suspended CNT *pn*-junction device consisting of carbon nanotubes grown over two gate electrodes buried under a dielectric oxide separated by a small trench 0.5 $\mu$m wide.[19,20] Later in 2011, Lee's group measured a series of bright exciton peaks through photocurrent spectroscopy and calculated the quantum efficiency and captured cross section of the excitonic transitions of these *pn*-junction devices.[21,22] Minot's group were able to identify chiralities through photocurrent spectra using suspended CNT devices with a single gate.[23] Zwiller's group reported the polarization dependence of dual-gate suspended CNT *pn*-devices.[24] Later, they separated two different mechanisms for the photocurrent generation process. Namely, the photothermal effect dominates in metallic CNTs, while the photovoltaic effect dominates in semiconductor CNTs.[25] On the contrary to Zwiller's theory, Steele's group argued that the photothermal effect also plays a role in semiconductor CNTs and is doping dependent.[26] Despite these previous studies, there have been no reports, to date, on the *gate dependence* of exciton and free carrier peaks in the photocurrent spectra of an individual suspended CNT *pn*-junction devices.

In the work presented here, we measure the photocurrent spectra of individual suspended CNTs as a function of the applied *pn*-junction gate voltages (i.e., $V_{g1} = -V_{g2}$). From over 100 devices fabricated and 10 devices measured, only individual, suspended CNTs that exhibit rectifying behavior that is not dominated by Schottky contacts are selected for further study. This is particularly difficult to achieve because of the high Schottky barriers for electrons at the Pt contacts, which tend to dope the entire nanotube *p*-type under all gating conditions. Several steps are taken to ensure that the active charge separation region of these *pn*-junctions is suspended off the substrate in a region away from the contacts,

 

including reversible rectifying *I-V* curves (i.e., *pn* and *np* configurations) and spatial mapping of the photocurrent, as described below. By studying the gate voltage dependence of photocurrent spectra of individual nanotubes, we are able to distinguish exciton from free particle excitations.

CNT samples are fabricated by etching a 4 $\mu$m wide, 500 nm deep trench in a $Si/SiO_2/Si_3N_4$ substrate, as described previously.[27,28] Two 1 $\mu$m-wide Pt gate electrodes separated by 2 $\mu$m are deposited on the bottom of the trench, as shown in Figures 1(a) and 1(b). The CNTs are grown using chemical vapor deposition (CVD) at 850 °C with Fe and Mo catalysts and ethanol as the carbon feedstock. High bias transport measurements are taken with $V_{g1} = V_{g2}$ in an argon environment to determine whether the device is suspended, which is indicated by a region of negative differential conductance (NDC).[29] The value of the maximum current enables us to determine if the device is a single isolated CNT or a bundle, as established by Pop *et al.*[29] Individual suspended CNTs that pass these selection criteria are selected and wire-bonded for further characterization. Current annealing is performed in argon at a bias voltage of $\pm 1.4$ V in order to remove any surface contaminants, which cause electron–hole recombination, before photocurrent spectra are taken. It should be noted that current annealing greatly improved the photocurrent spectra of these devices. Scanning electron microscope (SEM) images are taken after all photocurrent measurements were completed to avoid amorphous carbon deposition by the electron beam. Photocurrent spectra are collected by illuminating our devices with a Fianium supercontinuum white light laser used in conjunction with a double monochromater to produce monochromatic light over the 450–1600 nm wavelength range (0.78–2.76 eV). In order to improve the signal-to-noise ratio, data were taken using a chopper and a lock-in amplifier. All measurements were taken at room temperature.

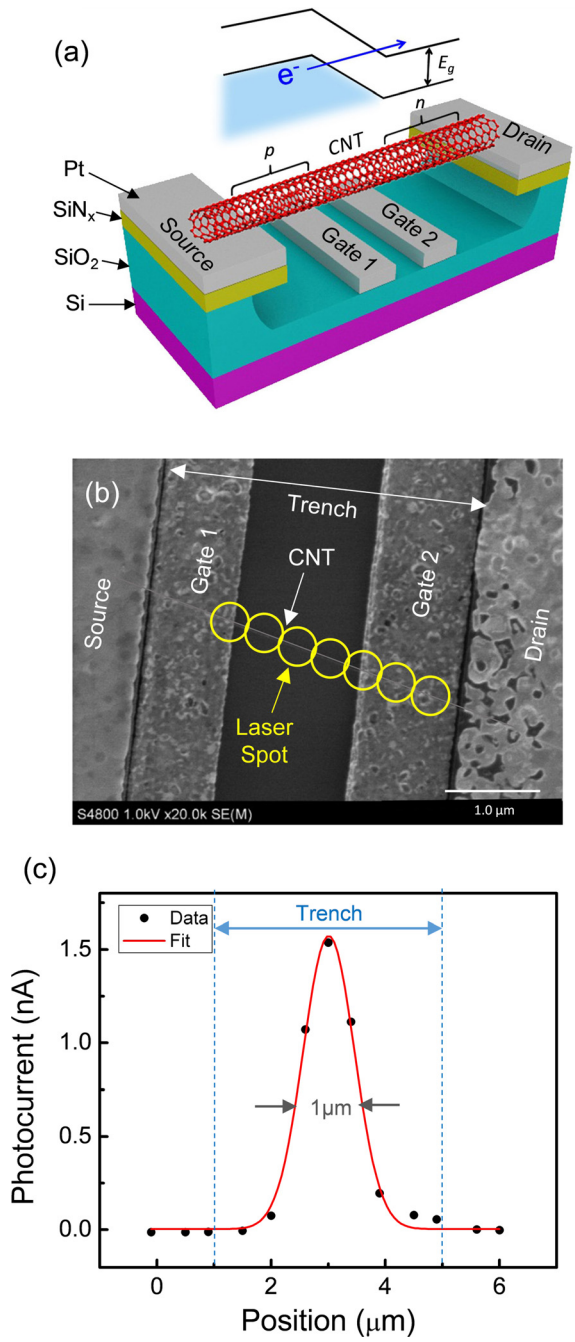


FIG. 1. (a) Schematic diagram illustrating the device structure of our CNT *pn*-junction devices. (b) SEM image of our device showing a single suspended CNT across the trench. (c) Spatial map of the photocurrent plotted along the length of the nanotube from the source to the drain electrode showing that the peak photocurrent is in the center of the suspended region away from the contacts.

Under *pn*-gating conditions (i.e., $V_{g1} = -V_{g2} = +9$ V), we observe rectifying behavior in the forward bias direction. When the gate voltages are reversed (i.e., $V_{g1} = -V_{g2} = -9$ V), we observe rectifying behavior in the reverse bias direction. See supplementary material[30] for the rectifying behavior characteristics. The reversibility of the rectifying behavior (i.e., achieving *pn* and *np*) is important in establishing that the rectifying behavior does not originate from a Schottky contact between the nanotube and the underlying metal contacts, as was the case in a vast majority of our devices, particularly for shorter devices. In order to further establish that the *pn*-junction is located away from the contacts in the suspended region of the nanotube, we spatially mapped the photocurrent along the length of the nanotube, as shown in Figure 1(c). Here, the maximum photocurrent clearly originates from the center of the CNT, rather than at the two Schottky contacts at the ends of the nanotube, as in previous studies.[23,31–34]

Figures 2(a) and 2(b) show the normalized photocurrent spectra taken from two different CNT devices (devices 1 and 2) under various *pn*-gating conditions with $V_{g1} = -V_{g2}$ and no applied source-drain bias. By increasing the gate voltage, we increase the doping concentrations in the *p*- and *n*-regions of the CNT and, hence, increase the built-in field at the *pn*-interface. Both devices 1 and 2 show peaks corresponding to a bright $E_{11}$ exciton peak and an $E_{11}$ free carrier band, approximately 0.4 eV higher in energy. From these spectra, we estimate the exciton binding energy to be 400 meV for device 1 and 360 meV for device 2, which agrees with previous reports in the literature.[1,35,36] The $E_{11}$ exciton peak intensities exhibit a strong gate dependence, while the $E_{11}$ free carrier peaks do not. Figure 2(c) shows the gate voltage dependence of these peak intensities for the two devices, which exhibit a clear gate dependence for the exciton peaks and gate independence for the free carrier peaks. In Figure 2(a), we see a splitting of the $E_{11}$ bright exciton peak around

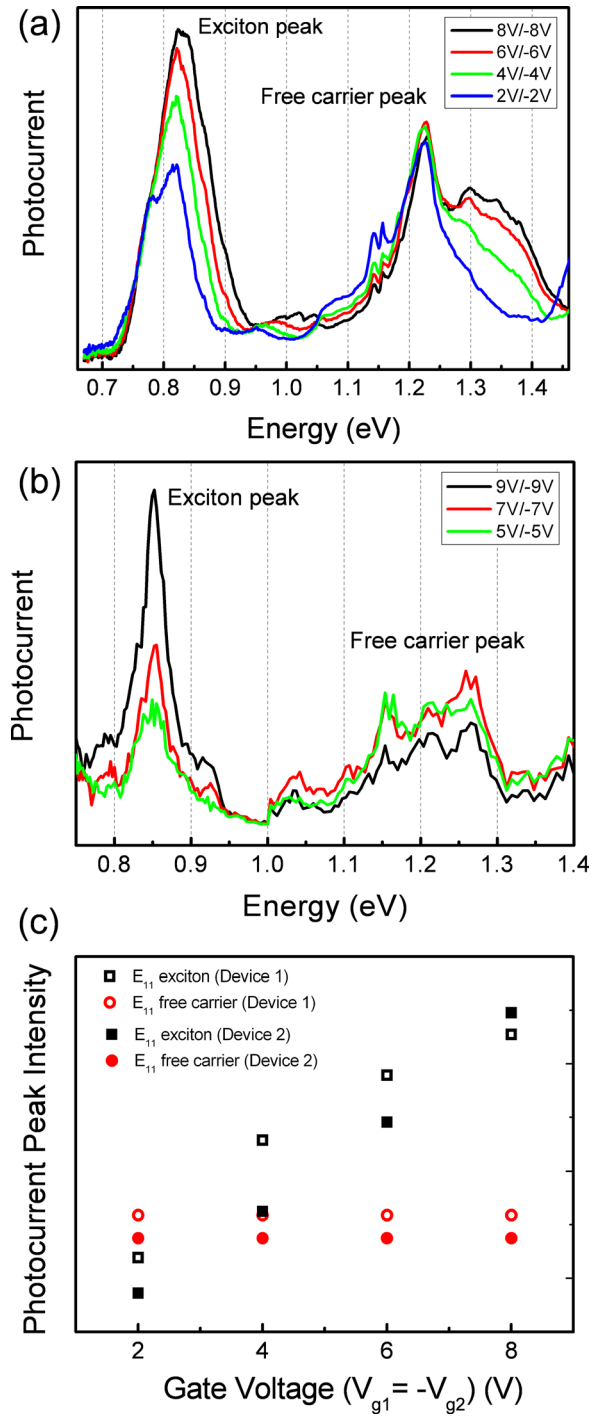


FIG. 2. Normalized photocurrent spectra taken from individual carbon nanotubes under various *pn*-gating conditions (i.e., $V_{g1} = -V_{g2}$) for (a) device 1 and (b) device 2. (c) Photocurrent peak intensities of the $E_{11}$ exciton and $E_{11}$ free carrier band plotted as a function of gate voltages. Hollow shapes are from device 1 and filled shapes are from device 2.

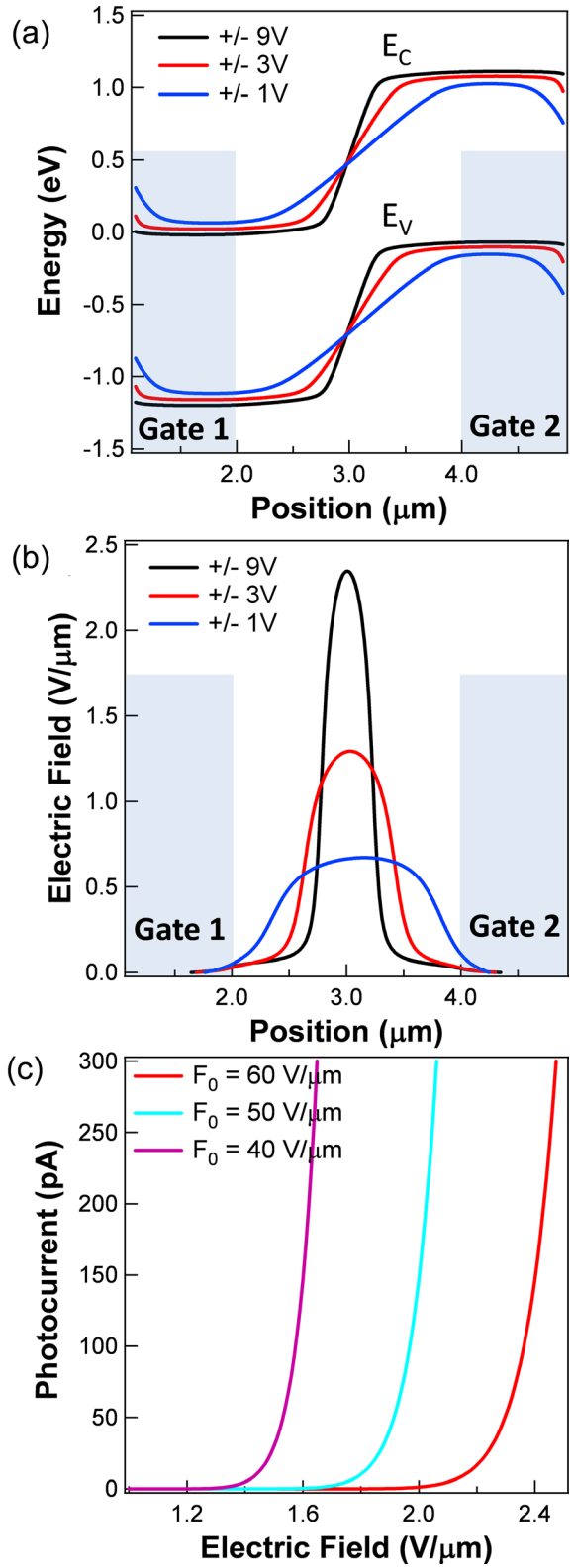


FIG. 3. (a) Simulated band diagrams for suspended carbon nanotube device with applied gate voltages of ±1 V, ±3 V, and ±9 V. (b) Electric field versus position profiles corresponding to the applied gate voltages in (a). (c) Estimated photocurrent considering phonon-assisted exciton dissociation for different critical fields $F_0$.

0.82 eV, on the order of 50 meV. Since a built-in field strength of 2 V/$\mu$m (see Figure 3) would only result in a Stark redshift of less than 0.5 meV,[37] we attribute this splitting to band gap renormalization (i.e., the doping dependence of the band gap), which can easily produce shifts of 50 meV.[27] Here, there are doped and undoped regions of the nanotube in the focal volume, which produce photocurrent at slightly different energies. This hypothesis is further corroborated by the fact that the splitting is most pronounced under low gating conditions (when the stark shift would be smallest) and when the undoped region is largest.

As a comparison, see supplementary material[30] for the photocurrent spectra taken from devices dominated by the

Schottky contacts. These photocurrent spectra were taken from a single-gate device with the laser focused on one of the metal contacts and a dual gate device that did not exhibit reversible rectifying behavior. Neither of the devices showed a gate dependence of the photocurrent peaks indicating that there is little control over the charge separating fields in devices dominated by Schottky contacts.

In order to obtain a more detailed understanding of the photocurrent generation mechanism in our *pn*-junction devices (Figure 2), we performed electrostatic simulations of these devices using the Sentaurus software package, which solves Poisson's equation iteratively to provide the self-consistent charge density profiles along the device. The corresponding conduction and valence band profiles are plotted in Figure 3(a) along the length of the CNT device. Here, the band offsets become more abrupt at higher applied gate voltages. The corresponding electric field profiles along the CNT device are plotted in Figure 3(b), and a maximum field strength of 2.3 V/$\mu$m is obtained under applied gate potentials of $\pm$9 V. To put this value of 2.3 V/$\mu$m in some theoretical context, we can divide the exciton binding energy 360–400 meV by the size of the exciton (approximately 5 nm)[35] to achieve a critical field of $F_o = 80$–100 V/$\mu$m required for the complete ionization of the excitons. Since this is almost two orders of magnitude higher than the built-in fields that are being applied experimentally, it is unlikely that this is the main mechanism of photocurrent generation. Since the photogenerated excitons must dissociate into free carriers in order to produce a photocurrent, the high binding energies in nanotubes suppress this photocurrent mechanism.

Perebeinos and Avouris calculated the phonon-assisted exciton dissociation rates in an applied electric field.[38] In this mechanism, the photogenerated exciton absorbs an optical phonon ($E_{ph} \sim 200$ meV), which lowers the effective binding energy (160–200 meV) and, hence, critical field for complete ionization ($F_o = 40$–50 V/$\mu$m). Following their approach, we can utilize a simple equation to quantitatively calculate the photocurrent, $I_{ph}$ = (exciton dissociation rate)$\times$(total CNT exciton population). First, the total exciton population in the CNTs is estimated as the (No. of absorbed photons per second) $\times$ (exciton lifetime), both of which are established for CNTs. Next, we calculate the phonon-assisted exciton dissociation rate using the following relation:[38]

$$\Gamma_0 = \alpha E_b \frac{F_0}{F} \exp\left(-\frac{F_0}{F}\right), \tag{1}$$

where $E_b$ is the binding energy, $F$ is the applied field, $F_o$ is the critical field, and $\alpha = 4.1$ is a constant. From the photocurrent spectra, we can estimate the exciton binding energy. Given the binding energy of the ground state (360–400 meV) and the excited state (160–200 meV), we can estimate the range of the excited state $F_o$ to be $\sim$40–50 V/$\mu$m, consistent with previously calculated values for this range of binding energies. These values allow us to then estimate the magnitude of the photocurrent via the following equation:

$$I_{Ph} = A \frac{P_{In}}{E_{Ph}} e\tau_{Ex} \frac{\Gamma_0}{\hbar}, \tag{2}$$

where $A$ is the absolute fraction of incident light absorbed by the CNT, $P_{In}$ is the incident power, $E_{ph}$ is the energy per photon, $e$ is the elementary charge, and $\tau_{Ex}$ is the exciton lifetime. Here, we assume that 5 $\mu$W of power (1% of the incident power) is absorbed at 800 nm incident photon wavelength.[22] The dissociation rate is a strong function of applied electric field and $F_o$. Here, for applied electric fields of 2 V/$\mu$m, the dissociation rate ranges from $\sim 10^{-9}$ meV to $10^{-5}$ meV. The exciton lifetime is 85 ps.[11,12] This then allows us to get order of magnitude estimates for the fields necessary to achieve the observed photocurrents ($\sim$100 pA). Figure 3(c) shows the expected photocurrent plotted as a function of electric field for various critical fields ($F_o$). For fields of about 1–2 V/$\mu$m, photocurrents on the order of 100 pA are obtained for excitons *when phonon-assisted exciton dissociation is considered*. Without the phonon-assisted excitation, the expected photocurrents at fields of 1–2 V/$\mu$m would be $< 10^{-60}$ A, with fields of 13–14 V/$\mu$m necessary to obtain photocurrents in the 1–100 pA range. Thus, we conclude that phonon-assisted exciton dissociation is the dominant mechanism leading to photocurrent here.

In conclusion, the photocurrent spectra of individual, suspended carbon nanotube *pn*-junctions show distinctive behavior for free particle optical transitions and excitonic transitions. The photocurrent generated by excitonic transitions is strongly dependent on the magnitude of the *pn*-doping, while the free particle photocurrent is gate independent. Here, the built-in potential of the *pn*-junction is required to separate the strongly bound electron-hole pairs of the excitons, while free particle excitations do not require field assisted charge separation. Theoretical estimates of the built-in fields and photocurrents generated in these *pn*-junctions indicate that phonon-assisted exciton dissociation is the dominant mechanism of photocurrent generation for the excitonic transitions.

This research was supported by DOE Award No. DE-FG02-07ER46376 (S.W.C.). A portion of this work was carried out in University of California Santa Barbara (UCSB) nanofabrication facility, part of the NSF funded National Nanotechnology Infrastructure Network (NNIN) network.

[1]G. Dukovic, F. Wang, D. Song, M. Y. Sfeir, T. F. Heinz, and L. E. Brus, "Structural dependence of excitonic optical transitions and band-gap energies in carbon nanotubes," Nano Lett. **5**, 2314–2318 (2005).
[2]S. M. Bachilo, M. S. Strano, C. Kittrell, R. H. Hauge, R. E. Smalley, and R. B. Weisman, "Structure-assigned optical spectra of single-walled carbon nanotubes," Science **298**, 2361–2366 (2002).
[3]A. Hogele, C. Galland, M. Winger, and A. Imamoglu, "Photon antibunching in the photoluminescence spectra of a single carbon nanotube," Phys. Rev. Lett. **100**, 217401 (2008).
[4]T. Mueller, M. Kinoshita, M. Steiner, V. Perebeinos, A. A. Bol, D. B. Farmer, and P. Avouris, "Efficient narrow-band light emission from a single carbon nanotube p–n diode," Nat. Nanotechnol. **5**, 27–31 (2010).
[5]T. Hertel, S. Himmelein, T. Ackermann, D. Stich, and J. Crochet, "Diffusion limited photoluminescence quantum yields in 1-D semiconductors: Single-wall carbon nanotubes," ACS Nano **4**, 7161–7168 (2010).
[6]I. Sarpkaya, Z. Y. Zhang, W. Walden-Newman, X. S. Wang, J. Hone, C. W. Wong, and S. Strauf, "Prolonged spontaneous emission and dephasing of localized excitons in air-bridged carbon nanotubes," Nat. Commun. **4**, 2152 (2013).
[7]M. J. O'Connell, S. M. Bachilo, C. B. Huffman, V. C. Moore, M. S. Strano, E. H. Haroz, K. L. Rialon, P. J. Boul, W. H. Noon, C. Kittrell, J. P.

Ma, R. H. Hauge, R. B. Weisman, and R. E. Smalley, "Band gap fluorescence from individual single-walled carbon nanotubes," Science **297**, 593–596 (2002).
[8]S. Y. Ju, W. P. Kopcha, and F. Papadimitrakopoulos, "Brightly fluorescent single-walled carbon nanotubes via an oxygen-excluding surfactant organization," Science **323**, 1319–1323 (2009).
[9]D. M. Harrah, J. R. Schneck, A. A. Green, M. C. Hersam, L. D. Ziegler, and A. K. Swan, "Intensity-dependent exciton dynamics of (6,5) single-walled carbon nanotubes: Momentum selection rules, diffusion, and nonlinear interactions," ACS Nano **5**, 9898–9906 (2011).
[10]S. Iijima, "Helical microtubules of graphitic carbon," Nature **354**, 56–58 (1991).
[11]S. Moritsubo, T. Murai, T. Shimada, Y. Murakami, S. Chiashi, S. Maruyama, and Y. K. Kato, "Exciton diffusion in air-suspended single-walled carbon nanotubes," Phys. Rev. Lett. **104**, 247402 (2010).
[12]J. Lefebvre, D. G. Austing, J. Bond, and P. Finnie, "Photoluminescence imaging of suspended single-walled carbon nanotubes," Nano Lett. **6**, 1603–1608 (2006).
[13]L. Cognet, D. A. Tsyboulski, J.-D. R. Rocha, C. D. Doyle, J. M. Tour, and R. B. Weisman, "Stepwise quenching of exciton fluorescence in carbon nanotubes by single-molecule reactions," Science **316**, 1465–1468 (2007).
[14]L. Lüer, S. Hoseinkhani, D. Polli, J. Crochet, T. Hertel, and G. Lanzani, "Size and mobility of excitons in (6, 5) carbon nanotubes," Nat. Phys. **5**, 54–58 (2009).
[15]J. J. Crochet, J. G. Duque, J. H. Werner, B. Lounis, L. Cognet, and S. K. Doorn, "Disorder limited exciton transport in colloidal single-wall carbon nanotubes," Nano Lett. **12**, 5091–5096 (2012).
[16]B. A. Ruzicka, R. Wang, J. Lohrman, S. Ren, and H. Zhao, "Exciton diffusion in semiconducting single-walled carbon nanotubes studied by transient absorption microscopy," Phys. Rev. B **86**, 205417 (2012).
[17]M. D. Anderson, Y.-F. Xiao, and J. M. Fraser, "First-passage theory of exciton population loss in single-walled carbon nanotubes reveals micron-scale intrinsic diffusion lengths," Phys. Rev. B **88**, 045420 (2013).
[18]D. O. Bellisario, R. M. Jain, Z. Ulissi, and M. S. Strano, "Deterministic modelling of carbon nanotube near-infrared solar cells," Energy Environ. Sci. **7**, 3769–3781 (2014).
[19]J. U. Lee, "Band-gap renormalization in carbon nanotubes: Origin of the ideal diode behavior in carbon nanotube p-n structures," Phys. Rev. B **75**, 075409 (2007).
[20]J. U. Lee, P. J. Codella, and M. Pietrzykowski, "Direct probe of excitonic and continuum transitions in the photocurrent spectroscopy of individual carbon nanotube pn diodes," Appl. Phys. Lett. **90**, 053103 (2007).
[21]A. Malapanis, D. A. Jones, E. Comfort, and J. U. Lee, "Measuring carbon nanotube band gaps through leakage current and excitonic transitions of nanotube diodes," Nano Lett. **11**, 1946–1951 (2011).
[22]A. Malapanis, V. Perebeinos, D. P. Sinha, E. Comfort, and J. U. Lee, "Quantum efficiency and capture cross section of first and second excitonic transitions of single-walled carbon nanotubes measured through photoconductivity," Nano Lett. **13**, 3531–3538 (2013).
[23]T. DeBorde, L. Aspitarte, T. Sharf, J. W. Kevek, and E. D. Minot, "Determining the chiral index of semiconducting carbon nanotubes using photoconductivity resonances," J. Phys. Chem. C **118**, 9946–9950 (2014).
[24]M. Barkelid, G. A. Steele, and V. Zwiller, "Probing optical transitions in individual carbon nanotubes using polarized photocurrent spectroscopy," Nano Lett. **12**, 5649–5653 (2012).
[25]M. Barkelid and V. Zwiller, "Photocurrent generation in semiconducting and metallic carbon nanotubes," Nat. Photonics **8**, 47–51 (2014).
[26]G. Buchs, S. Bagiante, and G. A. Steele, "Identifying signatures of photothermal current in a double-gated semiconducting nanotube," Nat. Commun. **5**, 4987 (2014).
[27]S.-W. Chang, K. Bergemann, R. Dhall, J. Zimmerman, S. Forrest, and S. B. Cronin, "Non-ideal diode behavior and band gap renormalization in carbon nanotube pn junctions," IEEE Trans. Nanotechnol. **13**, 41–45 (2014).
[28]A. W. Bushmaker, V. V. Deshpande, S. Hsieh, M. W. Bockrath, and S. B. Cronin, "Direct observation of Born−Oppenheimer approximation breakdown in carbon nanotubes," Nano Lett. **9**, 607–611 (2009).
[29]E. Pop, D. Mann, J. Cao, Q. Wang, K. Goodson, and H. Dai, "Negative differential conductance and hot phonons in suspended nanotube molecular wires," Phys. Rev. Lett. **95**, 155505 (2005).
[30]See supplementary material at http://dx.doi.org/10.1063/1.4928196 for rectifying behavior characteristics and Schottky contact photocurrent spectra.
[31]M. Freitag, Y. Martin, J. Misewich, R. Martel, and P. Avouris, "Photoconductivity of single carbon nanotubes," Nano Lett. **3**, 1067–1071 (2003).
[32]X. Qiu, M. Freitag, V. Perebeinos, and P. Avouris, "Photoconductivity spectra of single-carbon nanotubes: Implications on the nature of their excited states," Nano Lett. **5**, 749–752 (2005).
[33]A. D. Mohite, P. Gopinath, H. M. Shah, and B. W. Alphenaar, "Exciton dissociation and Stark effect in the carbon nanotube photocurrent spectrum," Nano Lett. **8**, 142–146 (2008).
[34]A. Mohite, J.-T. Lin, G. Sumanasekera, and B. W. Alphenaar, "Field-enhanced photocurrent spectroscopy of excitonic states in single-wall carbon nanotubes," Nano Lett. **6**, 1369–1373 (2006).
[35]C. D. Spataru, S. Ismail-Beigi, L. X. Benedict, and S. G. Louie, "Excitonic effects and optical spectra of single-walled carbon nanotubes," Phys. Rev. Lett. **92**, 077402 (2004).
[36]F. Wang, G. Dukovic, L. E. Brus, and T. F. Heinz, "The optical resonances in carbon nanotubes arise from excitons," Science **308**, 838–841 (2005).
[37]M. Yoshida, Y. Kumamoto, A. Ishii, A. Yokoyama, and Y. K. Kato, "Stark effect of excitons in individual air-suspended carbon nanotubes," Appl. Phys. Lett. **105**, 161104 (2014).
[38]V. Perebeinos and P. Avouris, "Exciton ionization, Franz-Keldysh, and stark effects in carbon nanotubes," Nano Lett. **7**, 609–613 (2007).